3. Plasma and Tritium Interactions

3.1 Effects of Simultaneous Exposure of Beryllium and Carbon-fiber-composite Targets to High-power Pulsed Deuterium Plasma Fluxes

M.I.Guseva[1], V.M.Gureev[1], L.S.Danelyan[1], B.N.Kolbasov[1,*], S.N.Korshunov[1], V.G.Stolyarova[1], V.I.Vasiliev[2], V.M.Strunnikov[2], V.V.Zatekin[3], V.S.Kulikauskas[3]

[1] *Russian Research Center "Kurchatov Institute", Kurchatov Sq., 1, 123182, Moscow, Russia*

[2] *Troitsk Institute of Innovative and Thermonuclear Studies, 142092, Troitsk, Moscow Region, Russia*

[3] *D.V.Skobeltsin Institute of Nuclear Physics, M.V. Lomonosov Moscow State University, 1 Building 2, Vorob'yovy gory, 119992, Moscow, Russia*

Abstract

The study deals with the microstructure, the chemical and phase composition and the relative atomic concentration of D/C+Be on the surfaces of carbon fiber composite and beryllium targets simultaneously irradiated by a flux of high-power pulsed deuterium plasma in experiments simulating plasma disruptions.

Introduction

In the course of JET experiments with carbon and beryllium divertor tiles it was found out that the Be/C atomic ratio in redeposited layers varied from 1.5 to <0.003 depending on the location of a tile [1]. The atomic ratio D/C+Be was the greatest (0.77-0.80) in Be-enriched deposits, but in general it also varied depending on the divertor area where a tile was used.

This study deals with the microstructure, chemical and phase composition and the D/C+Be relative content on the surfaces of carbon fiber composite (CFC) and beryllium targets simultaneously irradiated by a flux of high-power pulsed deuterium plasma in experiments simulating plasma disruptions.

* Corresponding author: Tel. +7-095-1967583; fax: +7-095-9470073.

E-mail address: kolbasov@nfi.kiae.ru (B,N, Kolbasov).

Experimental

Samples of Be and CFC UAM-92-5D were placed in the MKT electrodynamic accelerator [2] and exposed simultaneously to a flux of pulsed deuterium plasma with energy density of 900 kJ/m^2 and pulse duration of 60 μs. The plasma had a density of 10^{15} cm^{-3} and ion energy of up to 1-2 keV.

The beryllium target was placed in a recess on the CFC-target surface. The erosion products were collected on a monocrystalline Si-plate placed in the beam shadow zone parallel to the beam.

The JEOL scanning electron microscope was used for microstructure analysis of target surfaces exposed to 10 plasma pulses and the materials deposited on the Si-collector. The chemical composition of the surface layers was determined by Rutherford backscattering method using Van de Graaf accelerator in which 1.6 MeV H^+ ions backscattered at 170^0 were detected with a surface barrier detector. Deuterium distribution in irradiated targets was profiled using the elastic recoil detection method, in which a beam of He^+ ions with 2.2 MeV hit a specimen under study at a 15^0 angle to its surface. The recoil atoms were detected at 30^0 relative to the initial direction of the He^+ incident beam. The deuterium atomic concentration in absolute terms was determined by measuring the energy spectra of standard calibrating specimens.

The phase composition of the Be-target surface layer was studied by X-ray diffraction analysis using a small angle diffractometer.

Results

Surface topography of the Be-target upon exposure to a D-plasma pulsed flux is shown in Fig.1. One can see that a large number of pores emerged along the grain boundaries, grain surface is covered by droplets and there are cracks on the target surface along the grain boundaries. As regards the CFC-target microstructure (see Fig.2), the exposure to D-plasma has predominantly affected its pyrolytic graphite matrix (Fig.2a) which has cracked and flaked off, while the reinforcing CFC-fiber structure has largely been unchanged (Fig.2b). The droplets spread out over the surfaces of both targets are redeposited erosion products, as proved by their presence on the cracks. Essentially, all the droplets spread over the Be-target have annular halos composed of tiny particles (Fig.3) – an indication that the depositing particles

may have carried electric charges of opposite signs. The droplets on the CFC UAM-92-5D surface can be observed on the matrix (Fig. 4*a, b*) and at some ends of the reinforcing fibers (Fig. 4*c*), while the fiber cylindrical surfaces are essentially free of them (Fig. 2*b*). Furthermore, there are pores on some fiber ends. (Fig. 4*d*) One can also observe 15-400 nm in diameter droplets on the UAM-92-5D surface remote from the Be target (Fig. 4*b*).

Formation of droplets discovered on Be and CFC targets after their exposure to the powerful pulsed deuterium plasma is conditioned by the Be-atom return from a dense near-surface plasma onto the targets. Similar droplets were observed by the authors of paper [3] under Be-deposition in vacuum at temperatures above 300 °C. The authors of paper [4] determined that round crystallized droplets, 200-800 nm in diameter, are formed at the temperature of condensation above 300 °C. Nucleation of the droplets occurs in the near-surface vapour, but not on the surface of growing Be-crystals. The droplets from the beginning are small and very mobile. Executing Brownian motion over the surface and on it, they join with each other.

The size distribution histograms for erosion products deposited on the CFC-target (*a*) and the Si-collector (*b*) are presented in Fig.5. The size distribution of the erosion products on the CFC target shows two maxima – in the ranges of 50-80 and 100-200 nm – and indicates that the particles of all sizes have an integral density of ~1.42 x 10^9 cm^{-2}. Droplets discovered on the Si-collector have greater diameters (0.1-2 μm) than those deposited on the irradiated targets. Their size distribution maximum is in the range of 0.2-0.4 μm (Fig. 5*b*), meaning that only the smaller particles have returned to the target from plasma. The density of all the particles deposited on the Si-collector is ~2.69 x 10^6 cm^{-2}.

In the part of the Be-target surface bordering the CFC area, redeposited particles have formed a wavy pattern (Fig. 6). The density of redeposited particles found on the Be and UAM-92-5D targets is ~4.5 x 10^7 and ~6.95 x 10^7 per cm^{-2} respectively.

The Rutherford backscattering analysis of layers redeposited on the Be-target revealed the presence of Be, C and O atoms, whose concentrations near the surface were 39.0; 32.7 and 28.3 at.% respectively (Fig. 7). The mixed Be+C layer was ~30 nm thick. At the depth of ~100 nm the concentration of C-atoms reduced to ~10 at.%. A preliminary X-ray diffraction analysis revealed that the near-surface zone of mixed layers (~16 nm) contained, besides an amorphous component, polycrystalline phases

of Be-oxide (BeO) and Be-carbonate ($BeCO_34H_2O$). The ratio of the polycrystalline phases is 57/43.

Fig. 8 shows the distribution profiles of deuterium in mixed layers codeposited on Be and CFC targets. The deuterium integral concentration in them is the same – 6.4 x 10^{19} cm^{-2}. However, in the case of CFC, the deuterium distribution is uniform throughout the layer, while in the case of Be, this uniformity can only be observed in a narrow,~10 nm thick, near-surface layer.

The D/C+Be atomic concentration ratio in the Be+C mixed layers is 0.019. The results of JET experiments carried out to determine D-concentrations in mixed Be+C layers at different parts of the divertor equipped with Be and C tiles suggest that such a comparably low D-content can only be observed in Be-tiles doped with a very slight addition of C (with C/Be ratio of 0.003-0.01). Where Be/C rises to ~1.0-1.5, the D-retention is much higher, and D/C+Be-ratio reaches 0.15-0.2, that is, becomes an order of magnitude greater than in mixed layers with close ratio of Be to C atomic concentrations, occurring in experiments simulating plasma disruptions.

Conclusion

1. A simultaneous irradiation of beryllium and CFC by pulsed fluxes of D-plasma in experiments simulating plasma disruptions led to the formation of mixed 30-50 nm thick layers. The Be/C atomic concentration ratio in such a layer on Be-target was 1.19. A preliminary X-ray diffraction analysis revealed that the near-surface zone of mixed layers (~16 nm) contained, besides an amorphous component, polycrystalline phases of Be-oxide (BeO) and Be-carbonate ($BeCO_34H_2O$). The ratio of the polycrystalline phases is 57/43.
2. Cracks evolved along the grain boundaries in the Be-target and in the pyrolytic graphite matrix of the CFC-target. A large number of pores developed in the grain bulk in the Be target. In the UAM-92-5D target, the reinforcing fiber structure has remained unchanged.
3. On the Be and CFC surfaces, one can observe 15-400-nm Be-droplets that have flown back from plasma. Their size distribution profile peaks at 50-80 nm.
4. Size distribution histogram for particles deposited on the Si-collector has maximum in the range of 200-400 nm. The size of the erosion products reaches 2 μm.

5. Mixed layers formed on both Be and CFC targets contain small quantities of deuterium. The integral D-concentration in both of these layers is the same – 6.4×10^{19} cm^{-2}. The D/C+Be atomic concentration ratio in the mixed layers is 0.019, that is, about an order of magnitude less than that observed under exposure to stationary plasma. A low D-content in the mixed layers is probably due to an intense momentary heating of the targets by a high-power pulsed plasma flux (up to ~3,500 K).

References

1. J.P. Coad, N. Bekris, J.D. Elder *et.al.*, *J. of Nucl. Mater.* **290-293** (2001) 224-230.
2. S.N. Korshunov, M.I. Guseva, V.M. Gureev *et.al.*, *Proc. IEA Int. Workshop on Beryllium Technology for Fusion*. Mito, Japan, 1997, p.216.
3. L.S. Palatnik and A.I. Fedorenko, Physics of metals and physical metallurgy **17** (1964) 866 (in Russian).
4. I.I. Papirov and G.F. Tikhinskij, Physical metallurgy of beryllium, Atomizdat, Moscow, 1968 (in Russian).

Figure captions

Fig. 1. Surface topography of Be-target exposed to D-plasma.

Fig. 2. Microstructure of CFC-target exposed to D-plasma: *a* – matrix, *b* – reinforcing fibers.

Fig. 3. Droplets spread over Be-target surface.

Fig. 4. Droplets and pores on CFC-target surface: *a* – matrix, magnification 10000, *b* – matrix, magnification 40000; *c,d* - end faces of reinforcing fibers.

Fig. 5. Size distribution histograms for the erosion products deposited on the CFC-target (*a*) and on Si-collector (*b*).

Fig. 6. Surface microstructure of the Be-target part bordering the CFC-area.

Fig. 7. Chemical composition of a mixed layer formed on the Be-target: -Be, - O, • C.

Fig. 8. Deuterium distribution profiles for Be and CFC targets exposed to D-plasma: - Be, - UAM-92-5D.

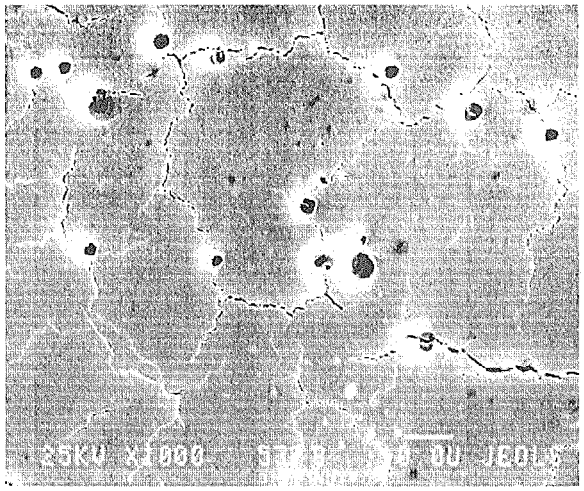

Fig. 1. Surface topography of Be-target exposed to D-plasma

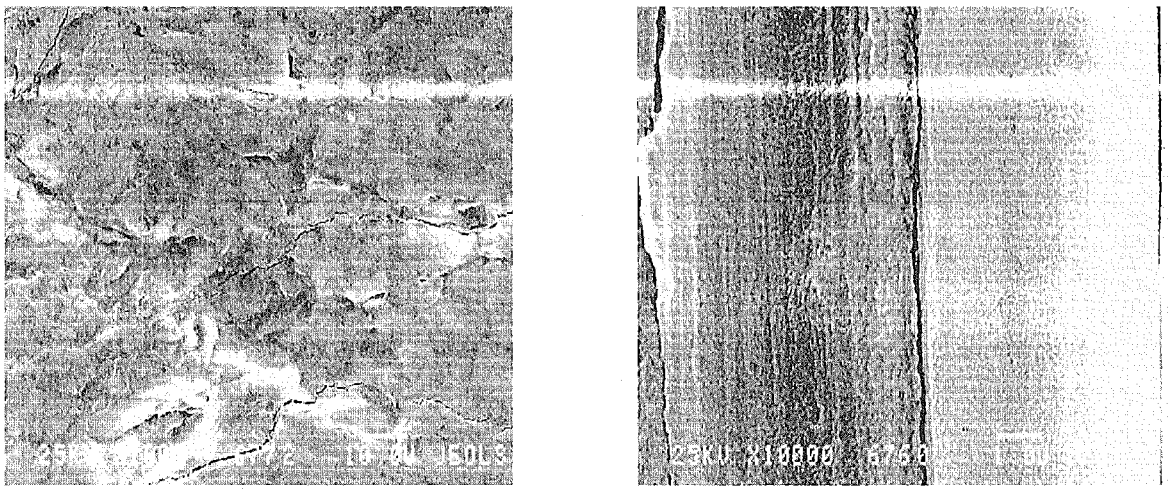

a *b*

Fig. 2. Microstructure of CFC-target exposed to D-plasma: *a* – matrix, *b* – reinforcing fibers.

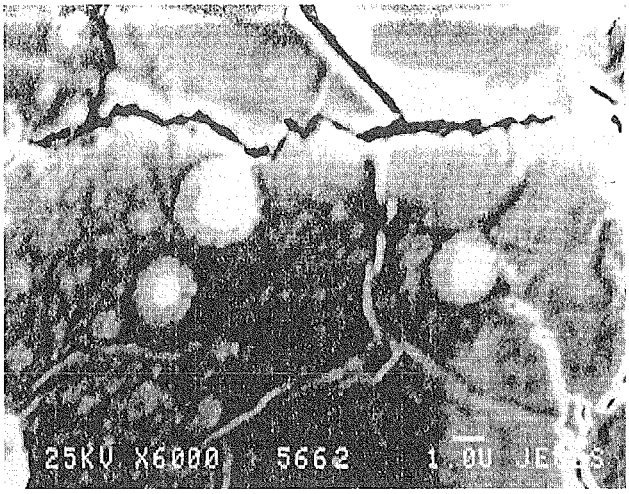

Fig. 3. Droplets spread over Be-target surface

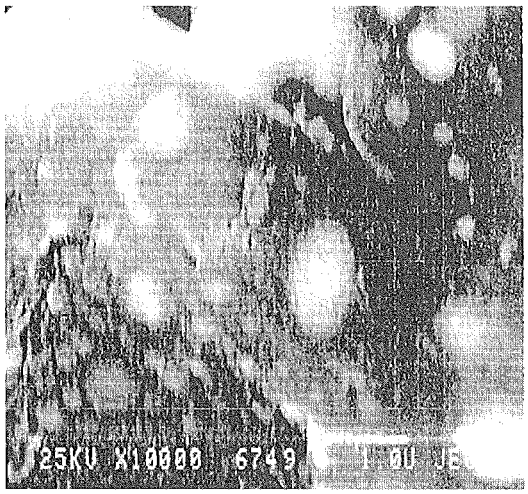

a

b

c

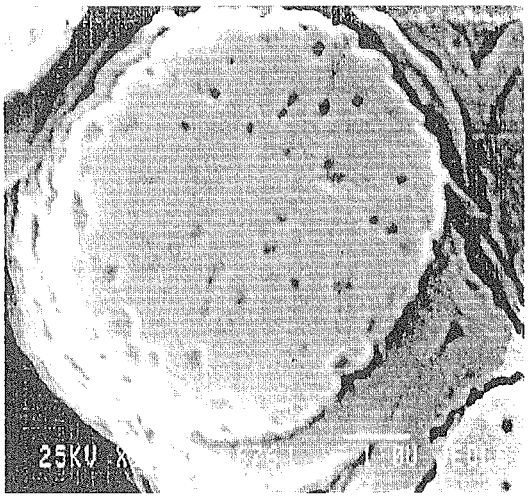

d

Fig. 4. Droplets and pores on CFC-target surface: *a* – matrix, magnification 10000, *b* – matrix, magnification 40000; *c,d* - end faces of reinforcing fibers.

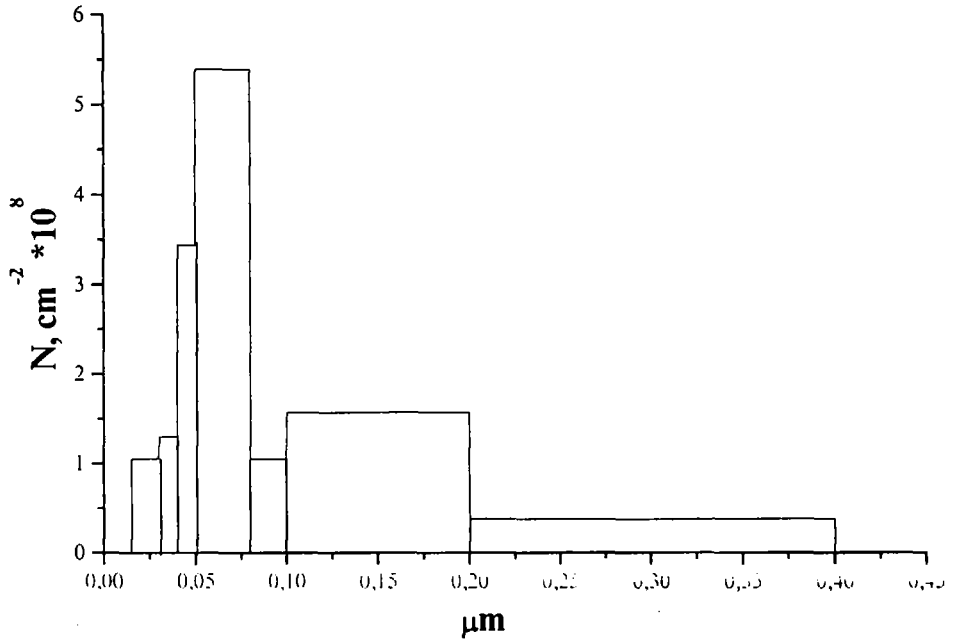

a

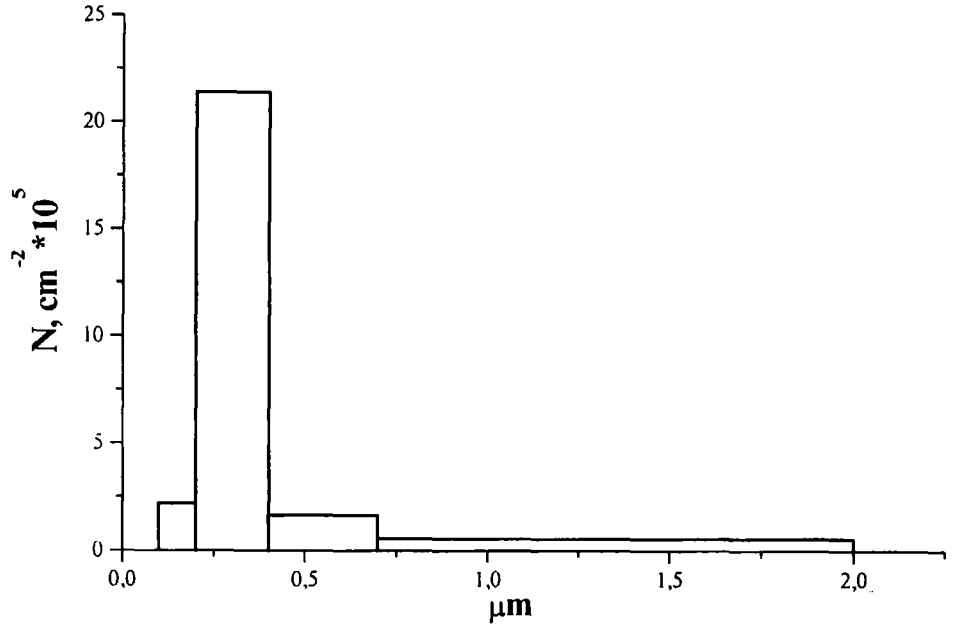

b

Fig.. 5. Size distribution histograms for the erosion products deposited on the CFC-target (*a*) and on Si-collector (*b*).

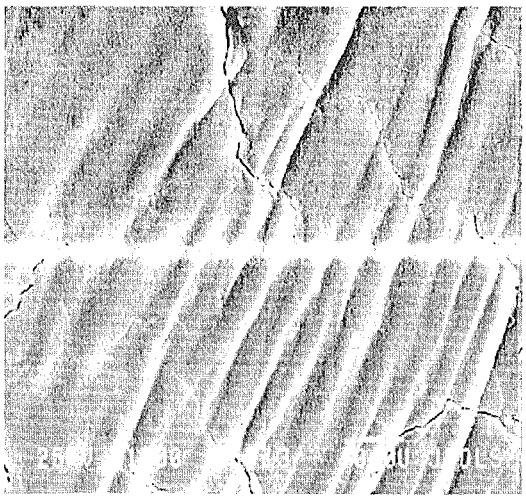

Fig. 6. Surface microstructure of the Be-target part bordering the CFC-area.

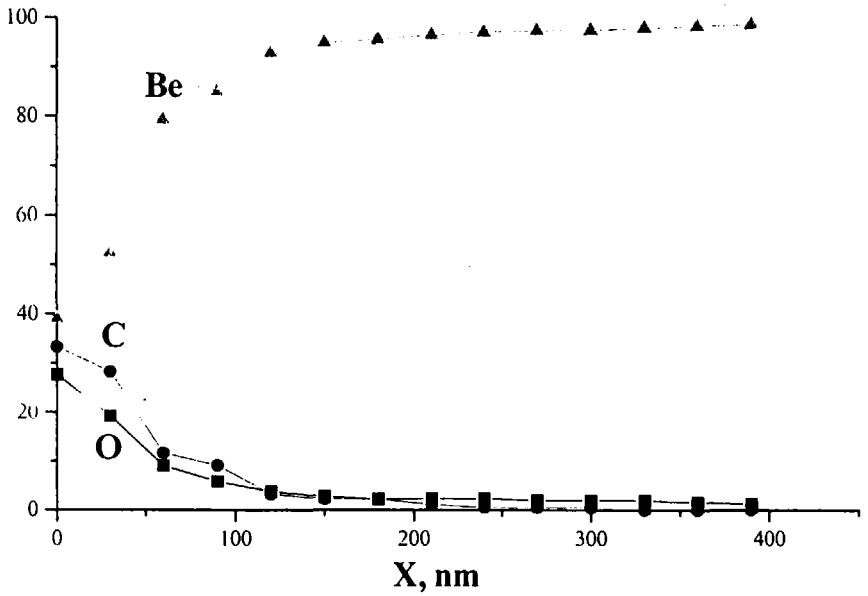

Fig. 7. Chemical composition of a mixed layer formed on the Be-target: -Be, - O, - C.

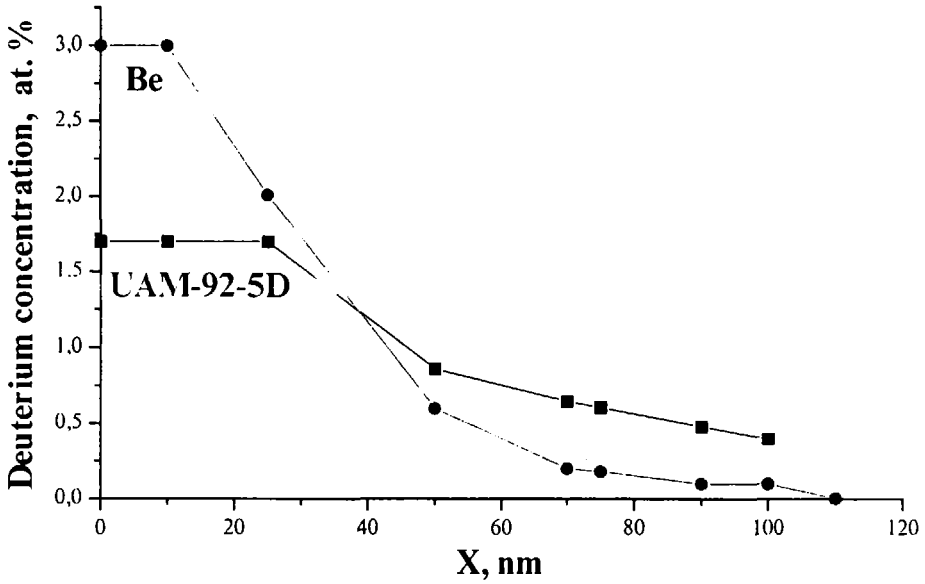

Fig. 8. Deuterium distribution profiles for Be and CFC targets exposed to D-plasma: - Be, - UAM-92-5D.